Quantitative determination of the phosphorus environment in lithium aluminosilicate glasses using solid-state NMR techniques

Pauline Glatz, Monique Comte, Lionel Montagne, Bertrand Doumert, Laurent Cormier

Quantitative determination of the phosphorus environment in lithium aluminosilicate glasses using solid-state NMR techniques

Pauline Glatz,[abc] Monique Comte,[a] Lionel Montagne,[b] Bertrand Doumert[d] and Laurent Cormier*[c]

[a] Corning European Technology Center, 7 Bis Avenue de Valvins, 77210 Avon, France

[b] Univ. Lille, CNRS, Centrale Lille, ENSCL, Univ. Artois, UMR 8181 – UCCS – Unite de Catalyse et Chimie du Solide, F-59000 Lille, France

[c] Sorbonne Universite, CNRS, Museum National d'Histoire Naturelle, IRD, Institut de Mineralogie, de Physique des Materiaux et de Cosmochimie (IMPMC), UMR 7590, 4 place Jussieu, 75005 Paris, France.

[d] Univ. Lille, CNRS, INRA, Centrale Lille, ENSCL, Univ. Artois, FR 2638 – IMEC – Institut Michel-Eugene Chevreul, F-59000 Lille, France

We investigated using solid-state NMR spectroscopy the short-range structural features in lithium aluminosilicate glasses with the addition of P_2O_5 and considering various Al_2O_3/Li_2O ratios. The phosphorus environment is determined quantitatively using ^{31}P Magic Angle Spinning NMR constrained by results obtained from $^{31}P–^{27}Al$ Multiple-Quantum Coherence-based NMR techniques. Phosphorus is mainly located as orthophosphate and pyrophosphate species in glasses with a low amount of Al_2O_3. These depolymerized units disappear with increasing Al_2O_3 content and a strong affinity of PO_4 tetrahedra for aluminum is revealed, which reduces phase separation. The local environments of framework (Si and Al) and charge-balancing (Li) cations are also studied through NMR experiments to assess the influence of P_2O_5 addition. The Si environment is mostly modified by the presence of P_2O_5 in glasses containing a low amount of Al_2O_3, with an increase of Q^4Si species in relation to phase separation phenomena observed in these compositions. Conversely, P_2O_5 addition does not have a significant influence on the ^{27}Al NMR response. ^7Li NMR spectra reflect a change in the structural role of Li when P_2O_5 or Al_2O_3 is added. The observed structural changes can be rationalized to improve our knowledge of the structure–property relationships, focusing, in particular, on phase separation and nucleation/crystallization processes that are strongly affected by the presence of P and the evolution of its local environment with composition.

1 Introduction

The Li_2O–Al_2O_3–SiO_2 (LAS) ternary system is of considerable interest for commercial glass-ceramics with a wide range of applications (cookwares, cooktops, precision optical materials, dental restoration etc.).[1] Slight modifications in composition may considerably change the sequence of phase formation. The addition of P_2O_5 is known to have a significant influence on phase separation, nucleation and crystallization, but the effective role of the nucleating agent of P is also strongly dependent on the Al_2O_3 content.[2–4]

With no Al_2O_3 or a small amount of Al_2O_3, the presence of P_2O_5 in Li_2O–SiO_2 glasses favors phase separation and tends to increase the crystal nucleation rate.[5–7] The characterization of the P environment is beneficial to address the role of P_2O_5, as recently established using ^{31}P NMR techniques.[4,8,9] Upon annealing of the parent glass, the P environment evolves with the formation of a highly disordered Li_3PO_4 and the con- comitant crystallization of Li_2SiO_3.[4,9] The crystallization of Li_3PO_4 appears only after further annealing.[8,10,11]

In aluminosilicates with increasing Al_2O_3 proportion, the P short range environment evolves considerably in the parent glasses with the disappearance of orthophosphate and pyro- phosphate units, PO_4^{3-} and $P_2O_7^{4-}$, respectively.[12] We have recently demonstrated that PO_4 tetrahedra are associated with AlO_4 tetrahedra in LAS glasses,[4] similar to those occurring in sodium aluminosilicate glasses.[12] As a result of this spatial P–Al proximity, nucleation is prevented or even delayed.[2,4]

A detailed knowledge of the phosphorus structural environment in glasses is thus essential to forecast its structural role in nucleation. However, the importance of this information extends beyond glass-ceramics. Indeed, depolymerized phosphorus environments such as orthophosphate species can induce bio- mineralization in bioactive glasses with a low amount of P_2O_5[13,14] or enhance conductivity in lithium silicophosphate glasses.[15,16] Alternatively, the co-doping of P and Al and the formation of P–O–Al linkages also modify glass properties, for instance by increasing rare-earth (RE) solubility, which influences RE distribution in optical fibers and luminescence properties of these materials.[17,18] Differences in the local environment of P with glass composition must thus be carefully determined.

A quantitative analysis of the P environment in LAS glasses has not been provided yet, despite the fundamental and commercial interests of this system. This is due to the difficulty in deconvoluting complex ^{31}P NMR spectra with several over- lapping contributions. Using $^{27}Al\{^{31}P\}$ Dipolar Hetero-nuclear Multiple-Quantum Coherence (D-HMQC) pulse sequence, the degree of association between aluminum and phosphorus can be assessed and full decomposition of ^{31}P NMR spectra can be obtained to determine the different P populations. The main objective of the present study is thus to present a complete characterization of the P local structure in LAS glasses with various Al_2O_3/Li_2O ratios. In addition, the effect of P_2O_5 addition on the aluminosilicate network and on the Li environment is explored using multi-nuclear (^{29}Si, ^{27}Al and ^{7}Li) solid-state NMR spectroscopy. The structural insights obtained in this investigation are discussed in terms of the competition for charge balancing cations between Al and P and their consequences on crystallization properties.

2 Experimental section

2.1 Materials

Glasses in the $Li_2O–Al_2O_3–SiO_2$ ternary system with 0 and 1 mol% P_2O_5 were prepared as described previously.[4] Analytical grade precursors Li_2CO_3 (Sigma Aldrich, 99%), Al_2O_3 (Merck, 99.9%), SiO_2 (Alfa Aesar, 99.5%) and $(NH_4)_2HPO_4$ (Sigma Aldrich, 98%) were mixed using an agate pestle and mortar, dried and melted in a platinum crucible at 1550 1C for 2 h. Then, the samples were quenched by dipping the bottom of the crucible into water. The glasses were ground and remelted again during 2 h at 1550 1C to ensure a good homogeneity.

The nominal and analyzed compositions are reported in Table 1. Glasses were synthesized along the 74 mol% SiO_2 isopleth, adding 0 or 1 mol% P_2O_5. A wide range of compositions is covered from Al_2O_3 (R = Al_2O_3/Li_2O) to peraluminous compositions (R = 1.3). The glasses are labeled as follows: LASR-Pn, where R is the ratio Al_2O_3/Li_2O and n is the mol% P_2O_5. Transparent, bubble free glasses were obtained, except for LAS0-P1, which was opalescent. For all samples, powder X-ray diffraction patterns confirm that the samples are amorphous. The glass compositions were examined by using an Electron Probe Micro-Analyser (EPMA, CAMPARIS, Sorbonne Universit´e, Paris, France) with a CAMECA SX-Five apparatus equipped with five Wavelength- Dispersive X-ray Spectrometers (WDSs) for SiO_2, Al_2O_3, and P_2O_5 and by performing Flame-Atomic Emission Spectroscopy (F-AES) using an Agilent AA280FS apparatus for Li_2O content. The EPMA instrument operates at 15 kV and 10 nA with a spot size of 5 mm. The standards for calibration were orthoclase for silicium and aluminum, and apatite for phosphorus. Compositions given in Table 1 are averaged over 20 measurements at different points and indicate that samples are homogeneous within the EPMA resolution limit.

2.2 Solid-state NMR

^{29}Si, ^{7}Li and ^{31}P MAS-NMR (Magic Angle Spinning Nuclear Magnetic Resonance) spectra were collected on a Bruker AVANCE I spectrometer operating at a magnetic field of 9.4 T. A 7 mm probe and a spinning frequency of 5 kHz were used for ^{29}Si. A 4 mm probe and a spinning frequency of 12.5 kHz were used for ^{31}P and ^{7}Li. The Larmor frequencies were 79.2, 155.5 and 161.9 MHz for ^{29}Si, ^{7}Li and ^{31}P respectively. For ^{29}Si, the pulse duration was 2 ms (p/5), and the recycle delay (rd) was 150 s, insufficient to ensure complete relaxation. For ^{7}Li and ^{31}P, the pulse durations were 1 ms ($\pi/8$) and 4.8 ms ($\pi/2$), respectively, and the rds were optimized at 40 s and 120 s to enable enough relaxation and get quantitative spectra. The chemical shifts are measured relative to tetramethylsilane (TMS) for ^{29}Si, relative to 85% H_3PO_4 solution for ^{31}P and relative to 1 M aqueous LiCl for ^{7}Li.

^{27}Al MAS-NMR spectra were recorded at 18.8 T on a Bruker AVANCE III spectrometer with a 3.2 mm probe at 20 kHz spinning speed. The Larmor frequency was 208.5 MHz. The pulse duration was 1 ms (p/10), and the rd was 2 s. The recycle delays have been defined to enable enough relaxation to get quantitative spectra. The ^{27}Al chemical shifts are referred to $Al(NO_3)_3$ solution.

Table 1 Analyzed compositions (mol%) obtained by EPMA and F-AES of the glasses investigated in this study. Nominal compositions are in parenthesis.

Errors are typically less than 0.3% relative to SiO_2, less than 0.7% relative to Al_2O_3, less than 3% relative to P_2O_5 and 2% relative to Li_2O and R = Al_2O_3/Li_2O

Glass	SiO_2	Al_2O_3	Li_2O	P_2O_5	R
LAS0-P0	74.4 (74.22)	0.3 (0.00)	25.3 (25.78)	0.01 (0.00)	0.01 (0.00)
LAS0-P1	73.6 (73.46)	0.2 (0.00)	25.1 (25.52)	1.1 (1.02)	0.01 (0.00)
LAS0.2-P0	75.7 (74.23)	4.6 (4.13)	19.7 (21.64)	0.02 (0.00)	0.23 (0.19)
LAS0.2-P1	74.3 (73.47)	4.2 (4.08)	20.7 (21.42)	0.8 (1.02)	0.20 (0.19)
LAS0.4-P0	74.5 (74.23)	7.4 (7.22)	18.1 (18.55)	0.01 (0.00)	0.41 (0.39)
LAS0.4-P1	75.0 (73.48)	7.6 (7.14)	16.4 (18.36)	1.0 (1.02)	0.46 (0.39)
LAS0.7-P0	73.6 (74.22)	10.8 (10.31)	15.6 (15.47)	0.01 (0.00)	0.69 (0.67)
LAS0.7-P1	73.8 (73.47)	10.2 (10.21)	15.0 (15.30)	1.0 (1.02)	0.68 (0.67)
LAS1-P0	74.0 (74.23)	13.2 (12.89)	12.8 (12.89)	0.003 (0.00)	1.03 (1.00)
LAS1-P1	73.7 (73.47)	13.0 (12.76)	12.5 (12.76)	0.79 (1.02)	1.04 (1.00)
LAS1.3-P0	74.1 (74.23)	14.7 (14.43)	11.2 (11.33)	0.01 (0.00)	1.32 (1.27)
LAS1.3-P1	75.0 (73.47)	14.6 (14.29)	9.4 (11.22)	0.96 (1.02)	1.55 (1.27)

The $^{27}Al\{^{31}P\}$ 2D map of the LAS0.4-P1 glass was edited using the Dipolar Hetero-nuclear Multiple-Quantum Coherence (D-HMQC) sequence[19] at 18.8 T on a Bruker AVANCE III spectrometer with a 3.2 mm HPAl probe operating at a spinning frequency of 20 kHz. The 3988 20 data points were acquired using a ^{27}Al selective 901–t–1801–t spin-echo. The ^{31}P channel was irradiated using 901pulseswitha1.1msrecouplingtimeusingtheSR4$^2_1$ sequence. Each t1 was recorded using 18432 scans with a rd of 0.5 s. D-HMQC data are based on dipolar interactions, which means that spatial proximities between nuclei are probed. The used recoupling time allows a distance of around 5 Angstrom to be probed. This technique is not quantitative since the efficiency of magnetization transfer between two nuclei depends on the considered coupling (maximal efficiency for certain couplings).

The Multiple Quantum Magic Angle Spinning (MQ-MAS) experiment on the LAS1.3-P1 glass has been performed using a shifted echo pulse sequence[20] followed by shear transformation during data processing. Excitation (1.5 ms) and reconversion (0.5 ms) pulses were optimized to obtain maximum intensity. A spinning frequency of 60 kHz and a 1.3 mm probe were used.

Spectral decompositions were performed using the DMFIT program.[21]

2.3 Scanning electron microscopy

Glasses were embedded in epoxy resin, then cross sections were polished and etched using hydrofluoric acid. The sample surfaces were coated with iridium (2 nm thick) and the micro- structures were observed using a SEM-FEG ZEISS Gemini SEM500, at an accelerating voltage of 5 kV. Observations have been made using an in-lens secondary electrons detector.

3 Results

3.1 Structure and microstructure of the aluminosilicate network

^{29}Si MAS-NMR spectra of the studied glasses are shown in Fig. 1. All the resonances are in a chemical shift range char- acteristic of silicon in four-fold coordination ($^{[4]}Si$).[22] Two well- separated peaks are observed for the Al_2O_3-free glasses (bottom curves), while only broad resonances are

observed when Al_2O_3 is added (R 4 0). In aluminosilicate glasses, the different $^{[4]}Si$ entities can be labelled $Q^n_{Si}(mAl)$ where n is the number of bridging oxygens (BOs) and m is the number of Al connected to Si via Si–O–Al linkages.

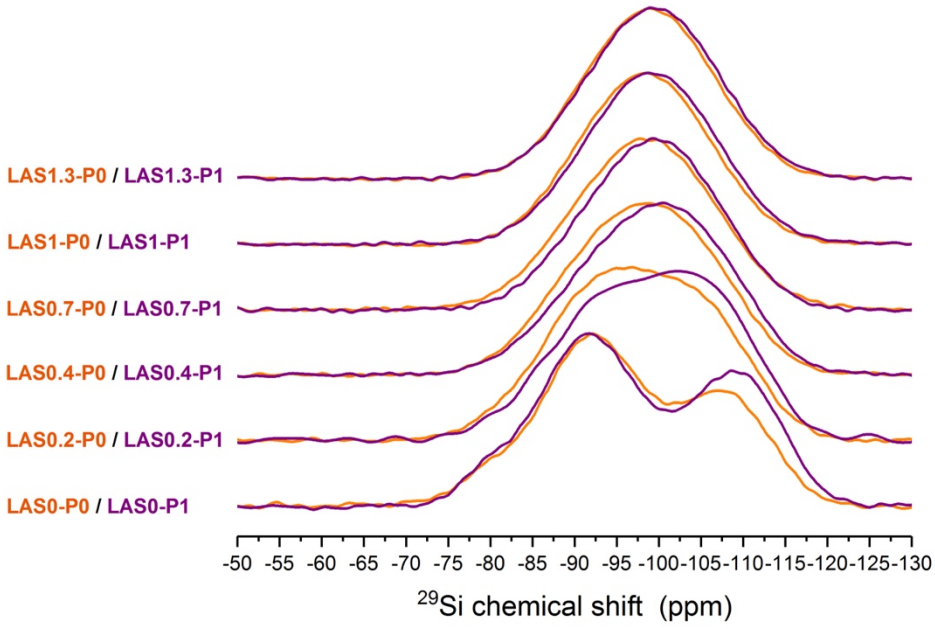

Fig. 1 ^{29}Si MAS-NMR spectra recorded at 9.4 T of LASR-Pn glasses, without P_2O_5 (orange) and with 1 mol% P_2O_5 (purple).

For the R = 0 glasses, two distinct peaks and one shoulder at high chemical shifts are observed. For LAS0-P0, these contributions can be attributed to $Q^4_{Si}(0Al)$ at 107.3 ppm, $Q^3_{Si}(0Al)$ at 92.0 ppm and $Q^2_{Si}(0Al)$ at 80.5 ppm.[23]

SEM images of the two R = 0 glasses are shown in Fig. 2. The LAS0-P0 sample exhibits a droplet-like phase separation with nodules of around 30 nm in size (Fig. 2a). These nodules are embedded in a darker phase. This latter phase seems less polymerized since it is more dissolved by acid etching. The presence of $Q^2_{Si}(0Al)$ species in the ^{29}Si NMR spectra in Fig. 1 (bottom) confirms the presence of less polymerized zones.

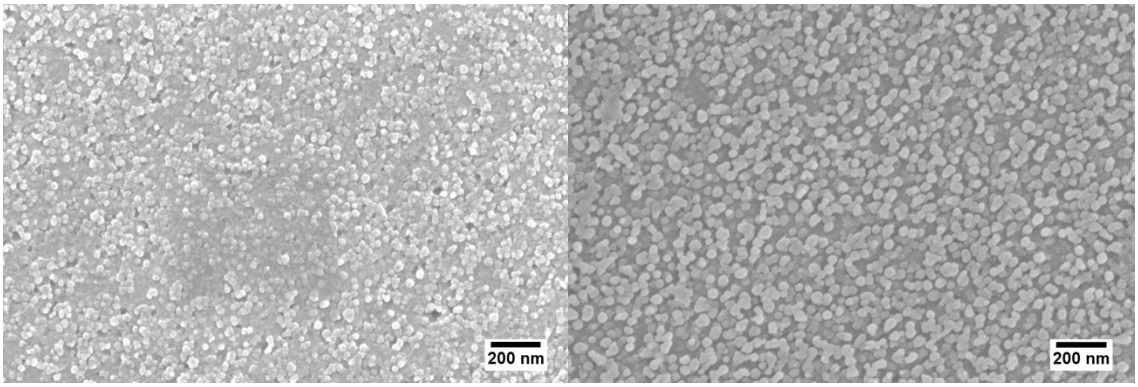

Fig. 2 SEM images of glasses: (a) LAS0-P0 and (b) LAS0-P1.

Addition of P_2O_5 into the R = 0 glass (LAS0-P1) results in a more negative chemical shift for the $Q^4_{Si}(0Al)$ contribution (from 107.3 ppm to 108.9 ppm, see Fig. 1), which is close to pure silica glass (around 110 ppm[24]). An increase of the phase separation is observed with the presence of nodules of around 40 nm in size (Fig. 2b), in agreement with the opalescence observed for this sample.

With the addition of Al_2O_3, from R = 0.2 to 1.3, we expect a higher number of $Q^n_{Si}(mAl)$ species with n values being mainly 3 or 4 and m between 1 and 4. The presence and overlap of these different species prevent the observation of distinct peaks and broad contributions with shoulders are observed on the ^{29}Si NMR spectra. The complete attribution and quantification of $Q^n_{Si}(mAl)$ population in ^{29}Si NMR spectra have been determined through multiple-quantum filtered INADEQUATE experiments in fully ^{29}Si-enriched aluminosilicate glasses[25] but this was not undertaken in the present study.

For R = 0.2, it is still possible to distinguish two contributions that are less polymerized (a more positive chemical shift) and more polymerized (a more negative chemical shift) species. The relative intensities of these two contributions are different in the glasses with and without P_2O_5. The introduction of Al_2O_3 increases the contribution of the most polymerized species and displaces the chemical shifts to lower values. Similar to the glasses with R = 0, P_2O_5 addition yields an increase in polymerization of the aluminosilicate network but no phase separation is observable via SEM in these glasses containing Al_2O_3. For R 4 0.2, the same trend is observed but the P_2O_5 influence is less visible on the spectra. In other terms, phosphorus has a stronger influence on silicate species and, possibly, on chemical disorder for glasses with a low amount of Al_2O_3.

^{27}Al MAS-NMR spectra of the studied glasses are displayed in Fig. 3. A peak in the region of 55–60 ppm indicates that aluminum is mainly present in tetrahedral coordination, $^{[4]}Al$. This peak position is consistent with the spectral region (56 to 64 ppm) that is commonly assigned to Al in fully polymerized (Q^4_{Al}) units in aluminosilicates.[26]

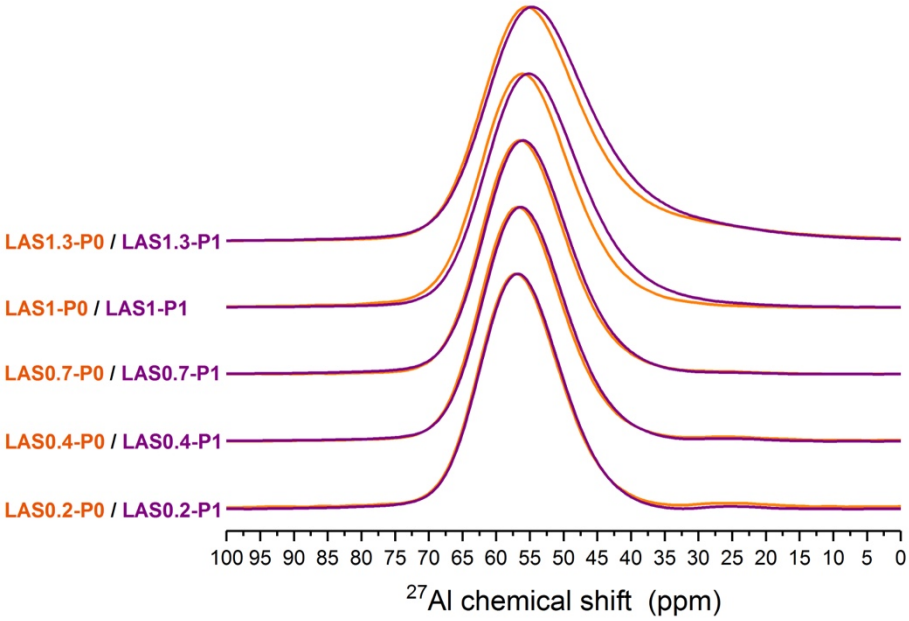

Fig. 3 ^{27}Al MAS-NMR spectra recorded at 18.8 T of LASR-Pn glasses, without P_2O_5 (orange) and with 1 mol% P_2O_5 (purple).

Despite that for R o 1, the excess of Li^+ cations ensures the charge compensation around (AlO_4) tetrahedra, a small peak near 25 ppm for LAS0.2-P1 and LAS0.4-P1 is detected, which could be due to minor amounts of five-fold coordinated sites, $^{[5]}$Al. This contribution has been detected earlier in per-alkaline earth aluminosilicate glasses.[27] For glasses with R Z 1, the contribution around 55–60 ppm becomes broader with a longer tail at low chemical shifts compared to glasses with R o 1. This is due to the lack of charge-balancing Li^+ cations, which induces the formation of $^{[5]}$Al and $^{[6]}$Al sites. These high coordinated species are expected when crossing the charge- balanced compositions (i.e. R = 1 line). The addition of P_2O_5 does not influence significantly the ^{27}Al spectra, indicating that P has a little effect on Al coordination. The changes associated with the Al_2O_3 content are emphasized in Fig. 4a, where stack plotted ^{27}Al MAS-NMR spectra are compared for glasses with increasing Al_2O_3 concentration. The small difference for glasses with R o 1 is observable as a slight shift of the peak maximum. For R Z 1, the tail at low chemical shifts is clearly observed.

The broadening cannot be ascribed uniquely to a larger amount of structural disorder when P_2O_5 or Al_2O_3 is introduced. Indeed, for the LAS1.3-P1 glass, the MQ-MAS spectrum has been recorded and is shown in Fig. 4b. The main contribution is $^{[4]}$Al but a small peak due to $^{[5]}$Al is also observable. As shown in Fig. 3, the increasing asymetry at low chemical shifts for the LAS1.3-P1 glass compared to the LAS1.3-P0 glass indicates slightly higher coordinated Al units in the presence of P_2O_5 but the broadening can also be due to interaction between aluminate and phosphate entities.

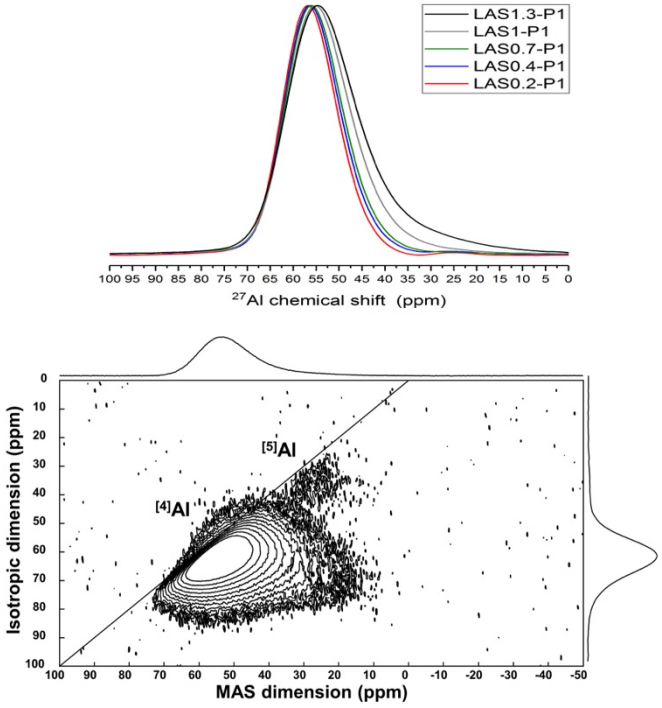

Fig. 4 (a) ^{27}Al MAS-NMR spectra recorded at 18.8 T of the LASR-P1 glass series. (b) ^{27}Al 3QMAS-NMR spectrum recorded at 18.8 T of the LAS1.3-P1 glass.

3.2 Lithium environment – ^{7}Li MAS-NMR

To explore the local Li environment, ^{7}Li MAS-NMR spectra were measured for the glass series (Fig. 5). They exhibit a single peak in the region near 0 ppm. NMR values are reported in Table 2.

For the LASR-P0 glass series without P_2O_5, the signal is shifted to more negative values when R increases (gravity centers shift from 0.18 ppm for LAS0-P0 to 0.58 ppm for LAS1.3-P0). In sodium aluminosilicates, it has been reported that Na–O bond lengths, and thus chemical shifts, are dependant on the modifying or compensating role of alkalis. When Na is a modifier, Na–O distances are shorter (higher covalency) than Na–O distances for a Na atom in a charge-balancing role (lower covalency).[28] A decrease in Na–O bond lengths yields a displacement of the chemical shift towards more positive values. In our case, gravity centers do not correspond to an isotropic chemical shift (due to quadrupolar interaction) but the observed shift of the resonances towards small chemical shift values can be attributed to a change of the Li^+ role from modifier to compensator near $[AlO_4]$ tetrahedra when R increases. It is also interesting to note that the width of the peak decreases significantly when R increases. This could be due to a decrease of dipolar Li–Li interactions as the Li_2O amount decreases when R increases.[29]

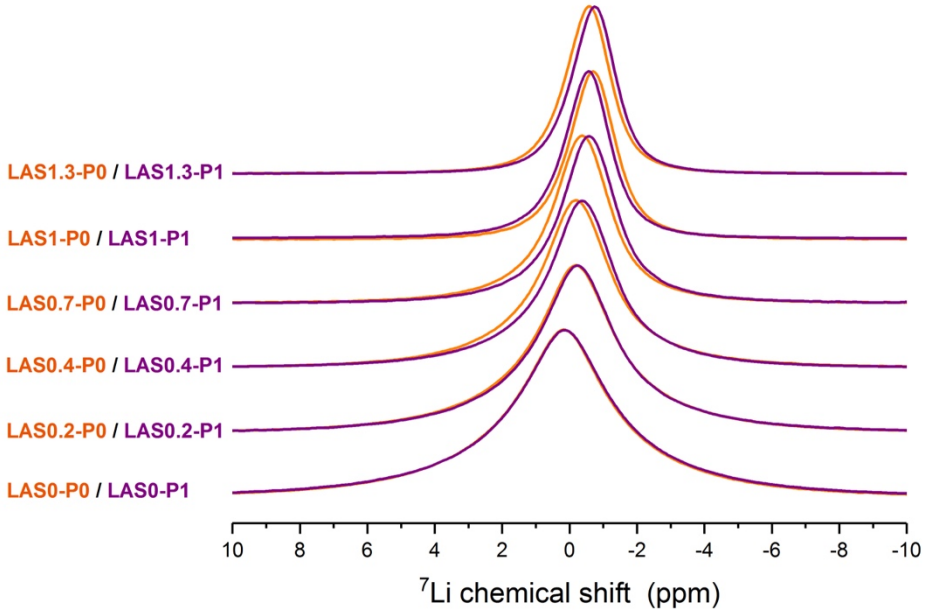

Fig. 5 ^{7}Li MAS-NMR spectra recorded at 9.4 T of LASR-Pn glasses, with- out P_2O_5 (orange) and with 1 mol% P_2O_5 (purple).

Table 2 Chemical shifts of gravity centers (in ppm, 0.05 ppm) and the Full Width at Half Maximum (FWHM in ppm, 0.05 ppm) of the peaks of ^{7}Li MAS-NMR spectra of LASR-Pn glasses. The Gaussian/Lorentzian ratio for simulation varied from 0 to 0.4 with R

R	Chemical shift (ppm)		FHWM (ppm)	
	0 mol% P_2O_5	1 mol% P_2O_5	0 mol% P_2O_5	1 mol% P_2O_5
1.3	-0.58	-0.74	1.57	1.50
1.0	-0.68	-0.58	1.62	1.55
0.7	-0.35	-0.56	1.98	1.90
0.4	-0.18	-0.35	2.43	2.29
0.2	-0.16	-0.22	2.82	2.77
0	0.18	0.17	3.40	3.44

The addition of P_2O_5 (LASR-P1 glasses) results in small modifications of the peak width (Table 2). A modification in the chemical shifts of the resonances is however observable since the peaks are displaced to more negative values for glasses with P_2O_5 compared with glasses without P_2O_5, except for R = 1. For 0 o R o 1, two explanations can be proposed for these differences. First, as evidenced by ^{29}Si MAS-NMR, the addition of P_2O_5 increases the network polymerization. Consequently, the number of NBOs decreases and the Li–O bonds are longer, which results in lower chemical shifts. Secondly, PO_4 entities attract mainly lithium to ensure their charge balance,[30] which results in weaker Li–O linkages due to the higher electronegativity of P compared with Si. Indeed, P–O bond strengths are stronger than Si–O ones, hence, antagonist bonds of (P)O–Li are weaker.

For R = 1.3, phosphorus is mainly surrounded by Al (see hereafter). As P atoms carry a 5+ charge, the Li cations are less involved to compensate the Al charge, which will be done by P. This results in weaker Li–O(Al) bonds, which means longer bonds, and thus explains the lower chemical shifts observed for ^{7}Li.

3.3 Phosphorus environment

3.3.1 Evolution of the local environment of phosphorus with R.

- Al-free glass, R = 0

The ^{31}P MAS-NMR spectrum of the glass LAS0-P1 is shown in Fig. 6b. Two resonances are observable at 9.3 ppm and at 1.3 ppm. They are assigned to orthophosphate units (PO_4^3, also noted as $Q^0_{P(0Al)_{glass}}$) and pyrophosphate units ($P_2O_7^4$, also noted as $Q^1_{P(0Al)_{glass}}$),[5,30] respectively. The chemical shift of the first resonance is close to that of crystalline Li_3PO_4 (10.1 ppm in ref. 31 and 9.6 ppm in our Li_3PO_4 reference sample in Fig. 6a, which can be noted as $Q^0_{P(0Al)_{crystal}}$). The second one is close to the two resonances of the two P crystallo- graphic sites in $Li_4P_2O_7$, $Q^1_{P(0Al)_{crystal}}$ (3.4 ppm and 5.9 ppm in ref. 32 and 3.8 ppm and 6.0 ppm in our $Li_4P_2O_7$ crystalline sample in Fig. 6a). The decomposition of the glass spectrum using these two contributions $Q^0_{P(0Al)_{glass}}$ and $Q^1_{P(0Al)_{glass}}$ is shown in Fig. 6b. In this LAS0-P1 glass, phosphorus is surrounded by Li^+ cations that are associated with NBOs on PO_4 units. The presence of orthophosphate and pyrophosphate species indicates that phosphorus is poorly associated with the silicate network in this glass without Al_2O_3.

- Al-bearing glasses, R 4 0

The ^{31}P MAS-NMR spectra of the LASR-P1 glasses are shown in Fig. 7. In the presence of aluminum (R 4 0), assignment of resonances is complex due to the presence of several species. These contributions overlap and lead to unresolved contributions for glasses with R Z 0.7. Addition of Al_2O_3 increases the signal intensity near 3 ppm and the chemical shift of the main resonance is shifted to negative values. Owing to the increase of Al^{3+} in glass compositions, we can attribute this shift to the interaction between PO_4^3 and AlO_4 species. Indeed, it has been reported[34] that the formation of aluminophosphate bonds induces a shift to a more negative value of ^{31}P NMR resonances. For instance, Dollase has reported a change of about 8 to 9 ppm for each additional Al in a solid solution of $Na_{(3-3x)}Al_xPO_4$.[34]

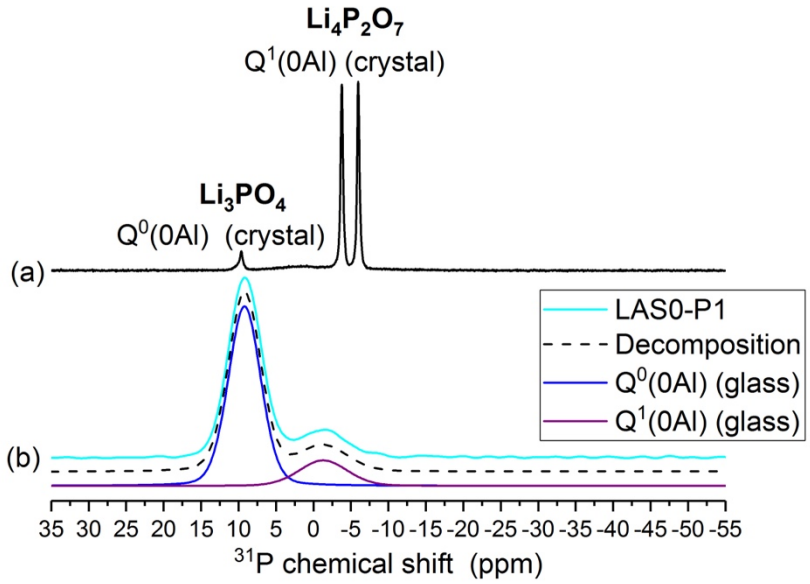

Fig. 6 ^{31}P MAS-NMR spectra recorded at 9.4 T of (a) sample containing Li3PO4 and Li4P2O7 crystalline phases provided by Khattech et al.[33] and (b) LAS0-P1 glass.

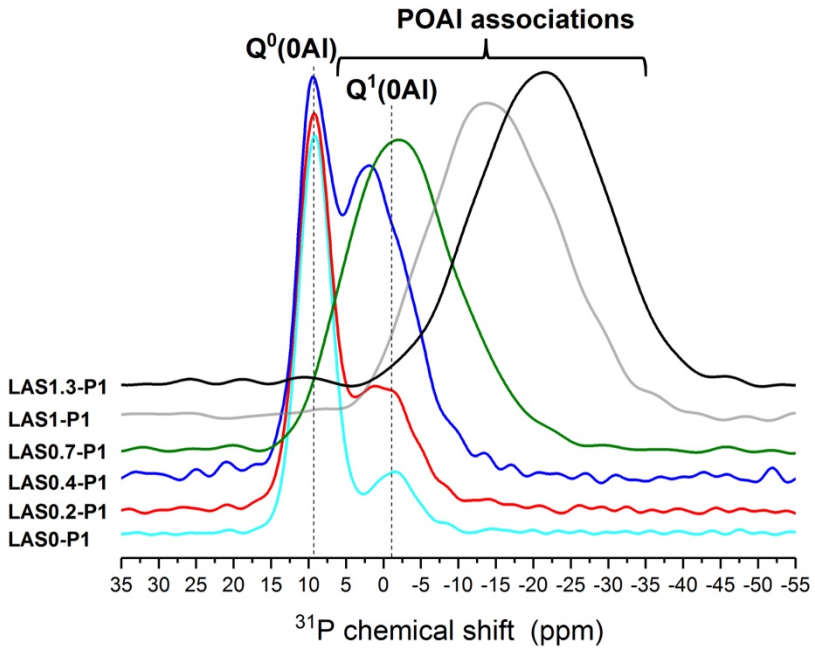

Fig. 7 ^{31}P MAS-NMR spectra recorded at 9.4 T of LASR-P1 glasses.

By analogy with silicate species, these aluminophosphate species can be written as $Q^nP(mAl)$ and are associated with POAl associations, as shown in Fig. 7. The presence of POAl associations has been evidenced in sodium aluminosilicate glasses[12,35,36] and, recently, in lithium aluminosilicate glasses[4] using ^{31}P–^{27}Al hetero- nuclear correlation NMR. In this latter study, $^{27}Al\{^{31}P\}$ D-HMQC spectra have been recorded for two glasses containing low and high amounts of Al_2O_3 (LAS0.2-P1 and LAS0.7-P1, respectively), showing that P–Al associations are present even in Al_2O_3-poor glasses, though in a minor content.

3.3.2 Phosphorus–aluminum interactions.

In the present paper, we recorded the $^{27}Al\{^{31}P\}$ D-HMQC spectrum for the LAS0.4-P1 sample that contains an amount of Al_2O_3 which is intermediate between those of LAS0.2-P1 and LAS0.7-P1 (Fig. 8). This experiment is presented here to explain our decomposition approach of the ^{31}P NMR spectra leading to quantitative information about the phosphorus environment for these glasses (see Table 3). The spectrum exhibits a through-space $^{27}Al\{^{31}P\}$ correlation signal that reveals spatial proximity between phosphate and aluminate species.

The projection of the 2D spectrum in the ^{31}P dimension is sketched as a dashed line in Fig. 8. It shows that the maximum intensity of the correlation is centered at 3.5 ppm in the ^{31}P dimension. This contribution does not take into account all the information under the curve, meaning that POAl associations are not the only entities, corroborating the result shown in Fig. 7. Indeed, two other species must be taken into account, meaning that orthophosphate and pyrophosphate species are still present.

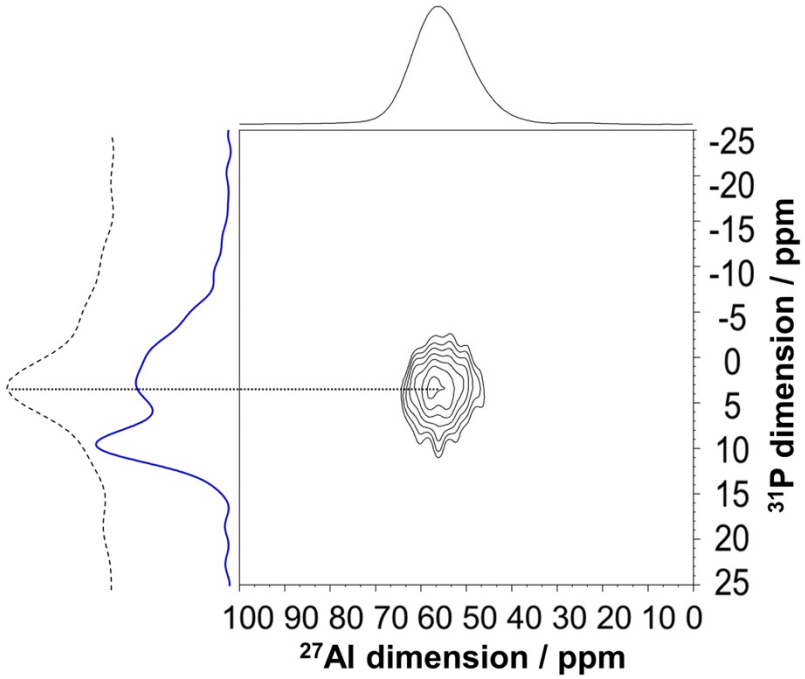

Fig. 8 $^{27}Al\{^{31}P\}$ D-HMQC spectrum recorded at 18.8 T of the LAS0.4P1 glass. The solid line on the top of the 2D map corresponds to the 1D ^{27}Al spectrum. The solid line on the left corresponds to 1D ^{31}P spectra and the dashed line is the ^{31}P projection of the 2D spectrum.

In their study of peralkaline sodium aluminosilicate com- positions, Toplis and Schaller[12] concluded the presence of individual PO_4^3 tetrahedra linked to the aluminosilicate frame- work with the replacement of one or two Na atoms by Al atoms. They observed a contribution at 7 ppm in their ^{31}P NMR spectra, which is attributed to a PO_4^3 ion linked to one Al atom. They concluded the presence of an orthophosphate species and not a pyrophosphate one as no correlation signal of the ^{31}P 2D spin exchange (^{31}P–^{31}P correlation) was observed for this 7 ppm contribution. This species can be noted as $Q^1P(1Al)$ and, similarly, in our lithium aluminosilicate glass, the contribution observed at 3.5 ppm can be attributed to $Q^1P(1Al)$. The projection of the $^{27}Al\{^{31}P\}$ 2D correlation in the ^{31}P dimension (dashed lines in Fig. 8) can be decomposed, which allows the determination of the isotropic chemical shift and linewidth for $Q^1P(1Al)$. With this informationandcontributionsof$Q^0P(0Al)$and$Q^1P(0Al)$deter- mined from the simulation of the 1D ^{31}P NMR spectrum of LAS0-P1 (the glass without alumina), a complete decomposition of the 1D ^{31}P NMR spectrum of LAS0.4-P1 has been obtained. The decomposition is shown in Fig. 9 and the associated Gaussian parameters are reported in Table 3. The fit parameters for the LAS0-P1 glass (Fig. 6) and for LAS0.2-P1 and LAS0.7-P1 glasses based on D-HMQC experiments presented earlier[4] are also reported in Table 3.

For the glass LAS0.4-P1 (decomposition of the spectrum in Fig. 9), the main contribution is $Q^1P(1Al)$ (32%) at the expense of $Q^0P(0Al)$ (31%) and $Q^1P(0Al)$ (26%) that are the main contributions for LAS0-P1 and LAS0.2-P1 (respectively 82% and 59% for $Q^0P(0Al)$, and 18% and 28% for $Q^1P(0Al)$). An additional Gaussian line at 3.5 ppm is required to obtain a satisfactory fit of the spectrum (Fig. 9). This contribution can be attributed to $Q^2P(2Al)$, a PO_4 entity linked to 2 Al atoms. This species is the most important one in the LAS0.7-P1 glass.[4] Simulation of the projection of the ^{31}P dimension of the $^{27}Al\{^{31}P\}$ D-HMQC spectrum enables, for LAS0.7-P1, the presence of another contribution at 13 ppm to be detected, which is attributed to $Q^3P(3Al)$(16%). In this latter glass, the species surrounded solely by Li cations are in very small amounts, only 4% (1% $Q^0P(0Al)$ and 3% $Q^1P(0Al)$), while P species connected to one Al or two Al are the main ones with 19% $Q^1P(1Al)$ and 61% $Q^2P(2Al)$.

It is also interesting to note that when R increases from 0 to 0.2, the amount of pyrophosphate groups increases from 18% to 28%. For R 4 0.2, the pyrophosphate contribution decreases due to the presence of POAl species.

Table 3 Chemical shifts (0.1 ppm), the Full Width at Half Maximum (FWHM) (0.1 ppm) and relative signal intensities (2%) of the different phosphate contributions of ^{31}P MAS-NMR spectra for glasses with R o 1

Sample	Q_P^0(0 Al)			Q_P^1(1 Al)			Q_P^1(0 Al)			Q_P^2(2 Al)			Q_P^3(3 Al)		
	δ_{iso} (ppm)	FWHM (ppm)	I (%)	δ_{iso} (ppm)	FWHM (ppm)	I (%)	δ_{iso} (ppm)	FWHM (ppm)	I (%)	δ_{iso} (ppm)	FWHM (ppm)	I (%)	δ_{iso} (ppm)	FWHM (ppm)	I (%)
LAS0-P1	9.2	5.1	82	-	-	-	-1.3	7.6	18	-	-	-	-	-	-
LAS0.2-P1	9.3	5.0	59	3.5	8.0	13	-1.3	9.0	28	-	-	-	-	-	-
LAS0.4-P1	9.6	4.8	31	3.5	8.0	32	-1.3	9.0	26	-3.5	12.0	11	-	-	-
LAS0.7-P1	9.3	5.0	1	3.5	8.0	19	-1.3	9.0	3	-3.5	12.0	61	-13.0	12.0	16

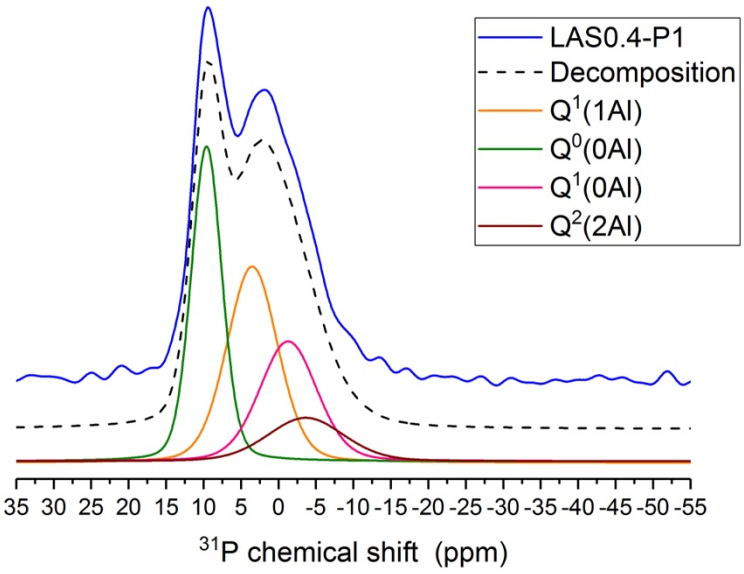

Fig. 9 ^{31}P MAS-NMR spectrum of the LAS0.4-P1 glass recorded at 9.4 T (solid blue lines) and its corresponding decomposition (dotted black lines). Individual contributions of phosphate species are shown in solid lines: Q^0P(0Al) (green), Q^1P(1Al) (orange), Q^1P(0Al) (pink) and Q^2P(2Al) (brown) and NMR parameters are reported in Table 3.

4 Discussion

4.1 Influence of P_2O_5 on the aluminosilicate network

The influence of P_2O_5 on the glass structure has been well- documented for lithium silicate glasses,[30,37] sodium alumino- silicate (NAS) glasses[12,38] and potassium aluminosilicate (KAS) glasses.[39] However, its effect on the structure of lithium alumino- silicate glasses is less investigated. ^{29}Si and ^{27}Al NMR spectra evolve with the R ratio. The addition of Al_2O_3 within the silicate network (increasing R) results in the presence of several Al atoms near Si atoms and various Q^nSi(mAl) species that cannot be deconvoluted without ^{29}Si isotopic enrichment.[25] The ^{29}Si NMR spectra are broadened by the overlap of these different Q^nSi(mAl) species. For the ^{27}Al NMR spectra, a peak broadening is observed with increasing R as the disorder increases in the $^{[4]}$Al surrounding and more $^{[5]}$Al sites are present.

The addition of P_2O_5 has a major macroscopic influence when considering glasses with a low Al_2O_3 concentration. Indeed, the composition without P_2O_5 (LAS0-P0, Table 1) is located in the immiscibility domain.[40,41] The SEM image (Fig. 2a) clearly shows a phase separation though the glass is macroscopically transparent. The phase separation is enhanced by the presence of P_2O_5 as revealed by SEM analysis (Fig. 2b) and a macroscopic opalescence becomes observable. Phosphorus oxide is well known to promote liquid–liquid phase separation in alkali silicate glasses.[6,42] Orthophosphate

and pyrophosphate units, which are both detected by ^{31}P NMR (Fig. 6b), are associated with four and three NBOs, respectively. Therefore, P is mainly localized in poorly-polymerized sites that scavenge Li^+ modifier ions to ensure charge balancing of PO_4^3 and $P_2O_7^4$. This explains the negative shift of the ^{29}Si resonance at 107.3 ppm. Indeed, this shift indicates the presence of more QSi^4 species when P_2O_5 is added: less Li cations are indeed available to promote NBO formation, which increases the silicate network connectivity. The effect of P_2O_5 insertion on the network connectivity can be rationalized using the following equations:[43]

$$6SiOM + P_2O_5 \rightarrow 2Q^0P3M + 3SiOSi \quad (1)$$

and

$$4SiOM + P_2O_5 \rightarrow Q^1P4M + 2SiOSi \quad (2)$$

with M being an alkali cation, here Li^+. The origin of increasing phase separation remains unclear. Clustering of orthophosphate species could lead to Si-rich and P-rich regions. Inhomogeneous atomic arrangements were established in a calcium phospho- silicate glass using ^{31}P spin-counting solid-state NMR that provided the evidence of well-separated phosphate clusters composed of five to six PO_4^3 units.[44] However, the phosphate clusters are not found in all glass compositions. Indeed, ^{31}P–^{31}P dipolar couplings obtained from NMR experiments revealed limited orthophosphate clustering in soda-lime silicate glasses, which suggests the incorporation of phosphorus atoms at interstitial positions within the open silicate network.[14,45] The phase separation could then be due to a displacement of the silicate composition towards the center of the immiscibility dome[7] due to preferential Li–P interaction, which induces network polymerization.

4.2 Evolution of the local phosphorus environment with composition

4.2.1 Dependence on the Al_2O_3 content. For LAS0.2-P1, the main environment around P is the one surrounded by Li, solely, i.e.$Q^0P(0Al)$(Fig.7andTable3),representing59%ofall phosphate species (0.59 0.82 2 = 0.97 mol% of P). This contribution represents 31% of the phosphate species (0.31 1.0 2 = 0.62 mol% of P) for LAS0.4-P1 and only 1% for LAS0.7- P1 (0.01 1.0 2 = 0.02 mol% of P). With the addition of Al_2O_3, the presence of POAl species has been experimentally evi- denced by NMR (Fig. 7 and 8). In LAS0.2-P1, POAl associations account for 13% of all phosphate species (only $Q^1P(1Al)$) while they represent 43% of the species for LAS0.4-P1 ($Q^1P(1Al)$ and $Q^2P(2Al)$) and 96% of the species for LAS0.7-P1 ($Q^1P(1Al)$, $Q^2P(2Al)$ and $Q^3P(3Al)$).

In Table 4, a calculation is reported that determines the percentage of Li_2O remaining within the silicate network con- sidering that all Al atoms are in tetrahedral sites and all P atoms are in orthophosphate units, i.e. the phosphate unit requiring the highest number of Li in its neighboring environ- ment. The results indicate that there is enough Li^+ to charge balance both AlO_4 tetrahedra and PO_4^3 entities, for all glass compositions. For LAS0.7-P1, the hypothesis that P atoms are in orthophosphate species can be confirmed and then a proportion of 1.8 mol% Li_2O is still available to act as a modifier and charge balance NBOs. This indicates that the Li_2O proportion does not drive the formation of the diverse P units and that there is a strong preference of phosphorus to bond with Al. POAl associations are thus favored in LAS glasses. Considering Pauling bond strength, s (in valence unit,

v.u.), defined as the quotient of the ionic valence over the coordination number, the P–O and Al–O bond strengths are 1.25 v.u. and 0.75 v.u., respectively. Therefore, the sum of bond strengths for an oxygen bonded to one P and one Al is 2 v.u. and the local electrostatic neutrality is satisfied.[46] Conversely, the presence of P–O–Si bonds has been rejected in aluminosilicate glasses due to the lack of Raman bands that are characteristic of the stretching vibration.[47]

Table 4 Table of analyzed compositions in mol% for LAS0.2-P1, LAS0.4-P1 and LAS0.7-P1 glasses and calculation of mol% Li2O remaining under the hypothesis that P2O5 inserts itself as Q^0P(0Al), i.e. only surrounded by lithium and not by Al, as observed by NMR

	LAS0.2-P1 mol%	LAS0.4-P1 mol%	LAS0.7-P1 mol%
SiO_2 analyzed	74.3	75.0	73.8
Al_2O_3 analyzed	4.2	7.6	10.2
Li_2O analyzed	20.7	16.4	15.0
P_2O_5 analyzed	0.8	1.0	1.0
Li_2O for charge balancing of AlO_4^-	4.2	7.6	10.2
Li_2O for charge compensating of phosphate species Q_P^0(0Al)	2.4 (3*0.8)	3.0 (3*1.0)	3.0 (3*1.0)
Li_2O remaining	14.1 (20.7-4.2-2.4)	5.8 (16.4-7.6-3.0)	1.8 (15-10.2-3.0)

4.2.2 Dependence on the nature of alkali. Previous studies have focused on aluminosilicate glasses with potassium[39] and sodium[12,38] as alkalis. In Table 5, we compare the influence of the nature of alkalis on the phosphorus species and proportions of each species, as determined by ^{31}P NMR in past studies and in the present one for a similar ratio R E 0.4.

It has been shown that the ratio of orthophosphate/pyropho- sphate species is strongly dependent on the cation field strength and the ratio increases in the order of Li^+ 4 Na^+ 4 K^+.[30] This agrees with the comparison shown in Table 5. This preferential order can be understood by the fact that Li^+ cations can accommodate more easily the three negative charges of a PO_4^3 orthophosphate unit while the low field strength cation K^+ is more efficient to charge balance the two negative charges on a PO_4 tetrahedron belonging to a pyrophosphate unit. There- fore, reaction (1) presented in paragraph 4.1 should be privileged for the LAS0-P1 glass.

Table 5 Evolution of phosphate species in aluminosilicate glasses with different alkali ions and with a ratio of R = M2O/Al2O3 E 0.4 obtained from ^{31}P NMR spectra and their decompositions

Sample name in the paper	KAS (ref. 39) P-9	NAS (ref. 12) NAPS70:4	LAS (this study) LAS0.4-P1
Cation field strength $\frac{z}{r^2}$ in Å^{-2} [48]	K^+	Na^+	Li^+
(with z valence and r cation ionic radius)	0.56	1.04	1.65
M_2O/SiO_2 with the M^+ alkali ion	0.17	0.33	0.22
Mol% of P_2O_5	1.7	3.6	1.0
Proportion of phosphate species according to ^{31}P NMR spectra	Q_P^1(0Al) mainly[a]	11% Q_P^0(0Al) 41% Q_P^1(0Al) 25% Q_P^1(1Al) 23% Q_P^2(2Al)	31% Q_P^0(0Al) 26% Q_P^1(0Al) 32% Q_P^1(1Al) 11% Q_P^2(2Al)

[a] No decomposition of the spectrum was done in this study[39]

In addition, we observe that POAl associations are favored for compositions with higher cation field strength. For the KAS system, Q^1P(0Al) is the main species. For the NAS system, POAl associations are present but the main species are pyrophos- phate units. On the contrary, for the LAS system,

$Q^nP(mAl)$ units are the main species. This preference in the LAS system can be explained by the fact that it is more favorable to form a $Q^nP(mAl)$ species from an isolated $Q^0P(0Al)$ species (which is the main phosphorus species in the composition without Al_2O_3) rather than from a $Q^1P(0Al)$ species. Indeed, in the latter case, a P–O–P bridge must be broken.

4.3 Effect of nucleation

It has been recognized that P_2O_5 has a nucleating role in lithium disilicate glasses.[49] Evidence of this nucleating role in more complex compositions with different cations and non-stoechiometric com- positions (with different SiO_2/Li_2O ratios)[4,9,47,50,51] has also been put forth. This structural role can be related to the formation of orthophosphate and pyrophosphate units either by the formation of phosphate clusters or by destabilizing the silicate network. It has been shown that a disordered Li_3PO_4 species acts as the first step for nucleation[4,9] and then crystallization of $Li_2Si_2O_5$, Li_2SiO_3 and quartz (a or b forms) in different volumes can be achieved with some

minimum amount of P_2O_5. In aluminosilicate glass compositions, surface crystallization is first detected.[2,4] This behavior can be related to the environment of phosphorus in the glass, since POAl associations impede disordered Li_3PO_4 species from appearing in the first nucleation steps. An evident correlation has thus been shown between the phosphorus environment in the parent glasses and its ability to behave as a nucleating agent.

5 Conclusions

The influence of P_2O_5 on the lithium aluminosilicate glass structure over a range of R = Al_2O_3/Li_2O ratios has been determined using ^{29}Si, ^{27}Al, ^{7}Li and ^{31}P NMR. At low P_2O_5 content, orthophosphate and pyrophosphate groups are the main species, which indicate a poor connection of PO_4 tetra- hedra with the silicate network. The depolymerized phosphate groups remove Li^+ ions from the silicate network, which favors phase separation. Based on the results of advanced solid-state MAS-NMR techniques, we have demonstrated the possibility to obtain a quantitative determination of P environments. These results clarify the structural evolution of P populations with increasing R and provide evidence for a high Al–P association in Al_2O_3-rich glasses. Nucleation by P_2O_5 can be obtained only when P atoms are not involved in Al–P association.

Conflicts of interest

There are no conflicts to declare.

Acknowledgements

We would like to acknowledge Anne Crochet (CETC, Corning SAS) for SEM images, and Peggy Georges and Sandrine Bercy (CETC, Corning SAS) for chemical analysis. The authors thank Ismail Khattech for providing the sample containing Li_3PO_4 and $Li_4P_2O_7$ crystalline phases. The ANRT is acknowledged for PhD funding (P. G.) under the CIFRE Contract 2015/0529. The authors thank the Chevreul Institute (FR 2638) for its help in the development of this work. The Chevreul Institute is supported by the ''Minist`ere de l'Enseignement Sup´erieur et de la Recherche'', the ''R´egion Hauts-de-France'' and the ''Fonds Europ´een de D´eveloppement des R´egions''.

References

1 M. Comte, in From Glass to crystal – Nucleation, growth and phase separation, from research to applications, EDP Sciences, 2017, pp. 375–386.

2 A. Arvind, A. K. Tyagi, R. Mishra, V. K. Shrikhande and G. P. Kothiyal, Phys. Chem. Glasses: Eur. J. Glass Sci. Technol., Part B, 2008, 49, 166–173.

3 Z. Zhao, J. Zhou, Y. Wang and M. Luo, Open Mater. Sci. J., 2011, 5, 45–50.

4 P. Glatz, M. Comte, L. Cormier, L. Montagne, B. Doumert and G. G. Moore, J. Non-Cryst. Solids, 2018, 493, 48–56.

5 D. Holland, Y. Iqbal, P. James and L. Bill, J. Non-Cryst. Solids, 1998, 232–234, 140–146.

6 W. Vogel, Glass chemistry, Springer-Verlag, Berlin Heidelberg, 1994.

7 A. Gaddam, H. R. Fernandes, D. U. Tulyaganov, M. J. Ribeiro and J. M. Ferreira, J. Non-Cryst. Solids, 1992, 481, 512–521.

8 C. Bischoff, H. Eckert, E. Apel, V. Rheinberger and W. Ho¨land, Phys. Chem. Chem. Phys., 2011, 13, 4540–4551.

9 S. Huang, Z. Zujovic, Z. Huang, W. Gao and P. Cao, J. Non- Cryst. Solids, 2017, 457, 65–72.

10 A. Ananthanarayanan, G. Kothiyal, L. Montagne and B. Revel, J. Solid State Chem., 2010, 183, 1416–1422.

11 W. Holand, E. Apel, C. van't Hoen and V. Rheinberger, Journal of Non-Crystalline Solids, 2006, 352, 4041–4050.

12 M.J. Toplis and T. Schaller,J.Non-Cryst.Solids,1998,224,57–68.

13 A. Tilocca and A. N. Cormack, J. Phys. Chem. B, 2017, 111, 14256–14264.

14 B. Stevensson, R. Mathew and M. Eden, J. Phys. Chem. B, 2014, 118, 8863–8876.

15 K. Rao, N. Baskaran, P. Ramakrishnan, B. Ravi and A. Karthikeyan, Chem. Mater., 1998, 10, 3109–3123.

16 V. Blache, J. Forster, H. Jain, O. Kanert, R. Ku¨chler and K. Ngai, Solid State Ionics, 1998, 113-115, 723–731.

17 M. Likhachev, M. Bubnov, K. Zotov, O. Medvedkov, D. Lipatov, M. Yashkov and A. Gur'yanov, Quantum Electron., 2010, 40, 633–638.

18 K. Bourhis, J. Massera, L. Petit, H. Ihalainen, A. Fargues, T. Cardinal, L. Hupa, M. Hupa, M. Dussauze, V. Rodriguez, C. Boussard-Pl´edel, B. Bureau, C. Roiland and M. Ferraris, Mater. Res. Bull., 2015, 63, 41–50.

19 J. Trebosc, B. Hu, J. Amoureux and Z. Gan, J. Magn. Reson., 2007, 186, 220–227.

20 D. Massiot, B. Touzo, D. Trumeau, J. Coutures, J. Virlet, P. Florian and P. Grandinetti, Solid State Nucl. Magn. Reson., 1996, 6, 73–83.

21 D.Massiot, F. Fayon,M. Capron, I. King, S. LeCalvé, B. Alonso, J.-O. Durand, B. Bujoli, Z. Gan and G. Hoatson, Magn. Reson. Chem., 2002, 40, 70–76.

22 H. Eckert, Prog. Nucl. Magn. Reson. Spectrosc., 1992, 24, 159–293.

23 H. Maekawa, T. Maekawa, K. Kawamura and T. Yokokawa, J. Non-Cryst. Solids, 1991, 127, 53–64.

24 M. Ed ́en, Annu. Rep. Prog. Chem., Sect. C: Phys. Chem., 2012, 108, 177.

25 J. Hiet, M. Deschamps, N. Pellerin, F. Fayon and D. Massiot, Phys. Chem. Chem. Phys., 2009, 11, 6935.

26 J. R. Allwardt, B. Poe and J. Stebbins, Am. Mineral., 2005, 90, 1453–1457.

27 D. Neuville, L. Cormier, V. Montouillout and D. Massiot, J. Non-Cryst. Solids, 2007, 353, 180–184.

28 F. Angeli, J.-M. Delaye, T. Charpentier, J.-C. Petit, D. Ghaleb and P. Faucon, J. Non-Cryst. Solids, 2000, 276, 132–144.

29 V. A. Vizgalov, T. Nestler, L. A. Trusov, I. A. Bobrikov, O. I. Ivankov, M. V. Avdeev, M. Motylenko, E. Brendler, A. Vyalikh, D. C. Meyer and D. M. Itkis, CrystEngComm, 2018, 20, 1375–1382. 30 R. Dupree, D. Holland and M. G. Mortuza, Phys. Chem. Glasses, 1988, 29, 18–21.

31 J. Ren and H. Eckert, J. Chem. Phys., 2013, 138, 164201.

32 S. Prabhakar, K. Rao and C. Rao, Chem. Phys. Lett., 1987, 139, 96–102.

33 H. Gmati-Ben Khaled, I. Khattech and M. Jemal, J. Chem. Thermodyn., 2013, 63, 11–16.

34 W. A. Dollase, L. H. Merwin and A. Sebald, J. Solid State Chem., 1989, 83, 140–149.

35 T. Schaller, C. Rong, M. J. Toplis and H. Cho, J. Non-Cryst. Solids, 1999, 248, 19–27.

36 G. Tricot, O. Lafon, J. Trebosc, L. Delevoye, F. Mear, L. Montagne and J.-P. Amoureux, Phys. Chem. Chem. Phys., 2011, 13, 16786–16794.

37 M. G. Mortuza, M. R. Ahsan, R. Dupree and D. Holland, J. Mater. Sci., 2007, 42, 7950–7955.

38 G. D. Cody, B. Mysen, G. S ́aghi-Szabo ́ and J. A. Tossell, Geochim. Cosmochim. Acta, 2001, 65, 2395–2411.

39 H. Gan and P. C. Hess, Am. Mineral., 1992, 77, 495–506.

40 Y. Kawamoto, J. Mater. Sci., 1985, 20, 2695–2701.

41 M. Tomozawa, V. McGahay and J. M. Hyde, J. Non-Cryst. Solids, 1990, 123, 197–207.

42 P. F. James, J. Mater. Sci., 1975, 10, 1802–1825.

43 B. Mysen and P. Richet, in Silicate glasses and melts, Elsevier, 2005, vol. 10, pp. 387–410.

44 F. Fayon, C. Du ́ee, T. Poumeyrol, M. Allix and D. Massiot, J. Phys. Chem. C, 2013, 117, 2283–2288.

45 R. Mathew, C. Turdean-Ionescu, B. Stevensson, I. Izquierdo-Barba,A.Garcia,D.Arcos,M.Vallet-RegiandM.Eden, Chem. Mater., 2013, 25, 1877–1885.

46 L. Pauling, J. Am. Chem. Soc., 1929, 51, 1010–1026.

47 M. Rampf, M. Fisch, G. Helsch, J. Deubener, C. Ritzberger, W. Höland and M. Dittmer, Int. J. Appl. Glass Sci., 2019, 10, 330–338.

48 A. Dietzel, Z. Elektrochem. Angew. Phys. Chem., 1942, 48, 9–23.

49 P. F. James, Y. Iqbal, U. S. Jais, S. Jordery and W. E. Lee, J. Non-Cryst. Solids, 1997, 219, 17–29.

50 T. J. Headley and R. E. Loehman, J. Am. Ceram. Soc., 1984, 67, 620–625.

51 W. Ho ̈land, V. Rheinberger, C. van't Hoen and E. Apel, Phosphorus Res. Bull., 2005, 19, 36–41.